

A MEMS Photosynthetic Electrochemical Cell Powered by Subcellular Plant Photosystems

Kien Bang Lam, Eric A. Johnson, Mu Chiao, and Liwei Lin, *Member, IEEE, ASME, Fellow*

Abstract—A microelectromechanical systems (MEMS) photosynthetic electrochemical cell (μ PEC) was demonstrated that harnesses the subcellular thylakoid photosystems isolated from spinach cells to convert light energy into electricity. Subject to light intensity of 2000 $\mu\text{mol photons/m}^2/\text{s}$, it generated an open circuit voltage (OCV) of 470 mV and a current density of 1.1 $\mu\text{A/cm}^2$ at 5.2 μV . In the dark, the μ PEC continued to yield power for a few minutes using reduced equivalents generated during illumination, generating 330 mV OCV and 0.1 $\mu\text{A/cm}^2$ with a 1 k Ω load. The output level is comparable to other MEMS biological fuel cells previously reported. The biosolar cell was bulk-micromachined from silicon and Pyrex substrates and assembled like a fuel cell in an anode-PEM-cathode configuration. This biosolar cell could have potential to serve as a power source for micro-scale devices like remote sensors. [1359]

Index Terms—Biological fuel cell, micropower source, photosynthesis, photosystems, solar cell.

I. INTRODUCTION

WE PRESENT a microelectromechanical systems (MEMS) photosynthetic electrochemical cell (μ PEC) that directly harnesses subcellular photosystems isolated from plant cells to perform bioconversion of light energy into electricity. The μ PEC has potential application as a power source for microscale and MEMS mobile devices such as remote distributed sensors [1], [2] and autonomous robots [3], [4].

This is the first demonstration of a MEMS PEC [5], [6], while previous work has concentrated on MEMS-based fuel cells [7], [8], microbial fuel cells [9], [10], and macro-scale PECs (reviewed later). The architecture of a macro-scale polymer electrolyte fuel cell was adapted to construct a MEMS micro-biofluidic device—with anode and cathode compartments bulk-micromachined in silicon and Pyrex substrates, to which reaction mixtures are delivered via bonded microfluidic needles.

Previous macroscale PEC work is reviewed here since it provides the basis for the present μ PEC. Tanaka *et al.* measured electrical output from cyanobacterium *Anabaena*

variabilis with HNQ as the redox mediator in both light and dark conditions [11], [12], concluding that their PEC generated electricity from both photosynthesis and catabolism of endogenous carbohydrates in the light and from catabolism alone in the dark. Yagishita *et al.* experimented with both *A. variabilis* and *Synechococcus* sp in their various PECs using HNQ as the mediator [13]–[18]. Output was 800 mV open circuit voltage (OCV), 320 $\mu\text{A/cm}^2$, and 1.4 mW from a PEC of area 7.2 cm^2 . Photoconversion efficiency ranged from 3.3% under sustained illumination to 0.2% when subject to illuminated charge and dark discharge cycles. Tsujimura *et al.* also used *Synechococcus* and 2,6-dimethyl-1,4-benzoquinone (DMBQ) as mediator to produce 800-mV open circuit voltage, 0.4 mA/cm^2 , and 0.19 mW/cm^2 , with photoconversion efficiency of 2% [19].

Whereas the previous PECs were powered by live whole-cell photosynthetic micro-organisms, Gross *et al.* demonstrated one of the earliest PECs using subcellular photosynthetic components [20]–[24]. They deposited either whole chloroplasts or isolated Photosystem I (PSI) particles onto one side (anode) of a cellulose triacetate filter. Under illumination and in the presence of flavin mononucleotide (FMN) as the electron acceptor in the anode compartment, this PEC yielded 640 mV OCV, 2.4 W/m^2 , and 1% efficiency.

Aizawa *et al.* immobilized manganese chlorophyll (MnChl) in a 4'-heptyl-4-cyanobiphenyl (HCB) liquid crystal film, which was attached to a Pt electrode and immersed in an alkaline solution [25]–[27]. Under irradiation, they found a negative potential shift of the electrode (anode). In contrast, when they immobilized magnesium chlorophyll (MgChl) in an *N*-(*p*-methoxybenzylidene)-*p*-butylaniline (MBBA) film in an acidic solution, they found a positive potential shift (cathode)-which, when paired with the MnChl-HCB electrode, formed a PEC.

In the pursuit of emulating photosynthetic membranes, various groups have isolated embedded reaction centers in phospholipids membranes. Skulachev *et al.* isolated reaction center complexes from *Rhodospirillum rubrum* and reconstituted them in proteoliposome planar phospholipids membranes. In the presence of certain redox mediators such as tetramethy-*p*-phenylenediamine (TMPD), they measured a trans-membrane potential of about 0.2 V [28]–[30]. Dutton and his group did related work [31], [32].

Janzen showed that reaction centers isolated from photosynthetic bacteria *Rhodospseudomonas sphaeroides* R-26 and dried as a film onto the semiconductor SnO_2 also were able to transfer electrons into SnO_2 [33], generating 80 mV OCV and 0.5 $\mu\text{A/cm}^2$. Illumination of chlorophyll produces in the

Manuscript received June 15, 2004; revised May 12, 2006. This work was supported in part by DARPA/MTO/BioFlips under Grant F30602-00-2-0566, by an ITRI Fellowship, and by the National Science Foundation under Grant ECS-0300542. Subject Editor A. J. Ricco.

K. B. Lam and L. Lin are with the Berkeley Sensor and Actuator Center, University of California, Berkeley, CA 94720 USA (e-mail: kblam@ocf.berkeley.edu; lwlin@me.berkeley.edu).

E. A. Johnson is with the Department of Biology, Johns Hopkins University, Baltimore, MD 21218 USA (e-mail: ejohn@jhu.edu).

M. Chiao is with the Department of Mechanical Engineering, University of British Columbia, Vancouver, BC V6T 1Z4, Canada.

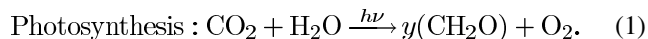
Color versions of Figs. 1–9 are available online at <http://ieeexplore.ieee.org>. Digital Object Identifier 10.1109/JMEMS.2006.880296

molecule both a positive hole (that can accept an electron) and an excited electron (that can be donated). With this in mind, Takahashi and Kukuchi proposed a galvanic cell in which: 1) the cathode compartment consisted of chlorophyll and naphthoquinone coated on an electrode in a solution of NAD^+ ; and 2) the anode compartment of chlorophyll and anthrahydroquinone coated on an electrode in ferricyanide solution. This cell produced 0.25-mV OCV and $8 \mu\text{A}/\text{cm}^2$. Haehnel *et al.* constructed a galvanic cell using isolated chloroplasts and various redox mediators interacting with PSI within the chloroplasts [34]–[36]. They measured as much as 220 mV OCV and $16 \mu\text{A}/\text{cm}^2$. Finally, Allen and Crane demonstrated an early PEC using isolated thylakoids [37].

II. THEORY

A. Photosynthesis

Photosynthetic organisms such as plants and certain bacteria capture solar energy to power the splitting of H_2O , releasing electrons that reduce CO_2 to produce carbohydrates (CH_2O). Carbohydrates are the biological fuel on which all nonphotosynthetic life on earth depends [38]



Equation (1) comprises a complex series of reactions, many of which occur in the subcellular photosystems (PSs) in higher plants. These PSs are networks of light-absorbing pigments (e.g., the green chlorophylls) and electron transporters that are arranged in two arrays, PSI and PSII (“Z-Scheme” of Fig. 1(c)). These networks are embedded in the membranes of structures known as thylakoids [Fig. 1(b)], which themselves are internal to organelles called chloroplasts, which in turn reside inside plant cells [Fig. 1(a)]. Under illumination, the pigments capture the energy of incident photons and funnel it to PSII to oxidize $2\text{H}_2\text{O}$ into O_2 . This splitting of H_2O releases electrons that then are transported from PSII to PSI along an electron transport chain composed of a series of membrane-bound enzyme complexes [38]. At the terminus of PSI, the electrons reduce NADP^+ into NADPH, a biological electron carrier [Fig. 1(c)].

Simultaneously, electron transport through the photosystems (i.e., PSII and PSI) pumps protons (H^+) across the thylakoid membrane from outside the thylakoid to inside. This creates a proton electrochemical gradient across the membrane (a proton-motive force) that powers the ATP synthase motor to produce ATP, the universal biological energy molecule (Fig. 1(b)) [38]. The energy transferred to NADPH and ATP by this “photo”-driven electron transport is then used to fuel the reduction of CO_2 into carbohydrates (CH_2O) by means of various anabolic pathways, thus forming the “synthesis” half of photosynthesis [38]. In the present implementation of the μPEC , however, the thylakoids and reaction mixtures were prepared (Section III) in such a way that neither NADPH nor ATP is produced because they are not essential to operation.

B. Photosynthetic Electrochemical Cell Operation

The μPEC generates electrical power, in essence, by harnessing electrons from the photosystems during the photo-

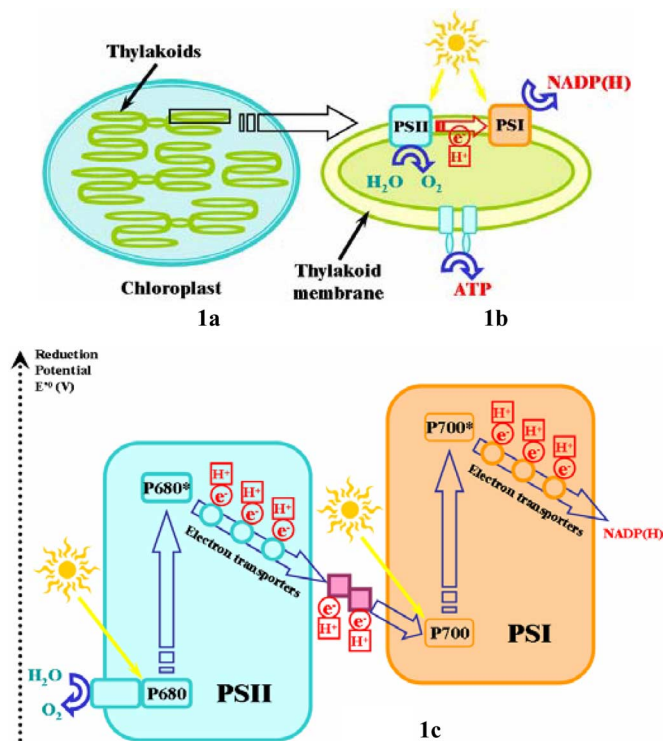


Fig. 1. (a) Chloroplast, an organelle inside plant cells. (b) Structures internal to chloroplasts, thylakoids have Photosystems I and II and ATP synthase embedded in their outer membranes. (c) Light energy powers photosynthesis “Z-Scheme,” which splits $2\text{H}_2\text{O}$ into O_2 , releasing electrons that are transported through the photosystems to reduce NADP^+ into NADPH.

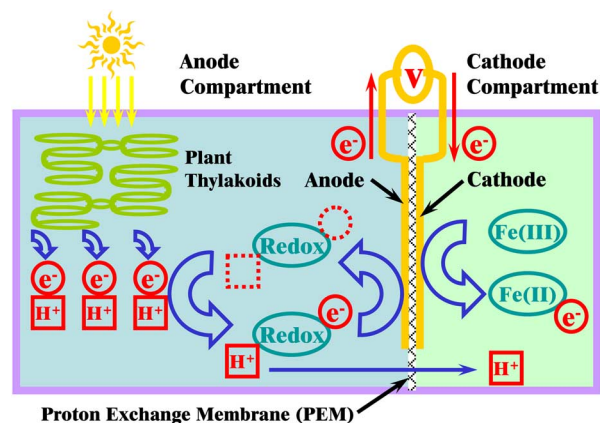


Fig. 2. During photosynthesis, electrons are transported through the photosystems in thylakoid membranes. Redox mediator PMS “siphons” these electrons (and protons, H^+) from the thylakoids and transports them to the anode. They then travel through an external load to the cathode, where they reduce oxidant Fe(III) or O_2 . Simultaneously, protons (H^+) diffuse from the anode compartment across the PEM into the cathode compartment.

to-driven phase of photosynthesis using the scheme shown in Fig. 2. Thylakoids were isolated from baby spinach—which interrupts the normal transport of electrons through the photosystems—and suspended in a buffer solution with the redox mediator phenazine methosulfate (PMS). The PMS “siphons” the electrons (e^-) and protons (H^+) being transported through the photosystems and transfers them to the anode (thus recovering PMS in the oxidized form). From the anode, the electrons flow through the external load (i.e., the device to

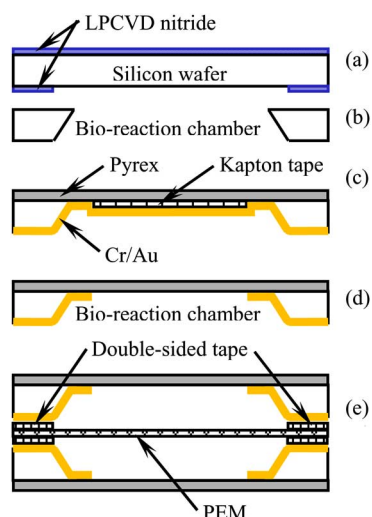
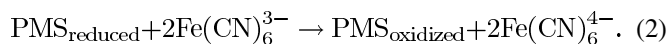


Fig. 3. Microfabrication and assembly. (a) Deposit LPCVD low-stress nitride and pattern wafer back side. (b) KOH-etch through wafer and strip nitride. (c) Anodically bond Pyrex wafer onto Si wafer front side. Apply Kapton tape on Pyrex in center of chamber. Evaporate Cr/Au 500/2000 Å. (d) Remove Kapton tape. (e) Compress PEM between two half-cells, with double-sided tape applied between Cr/Au and PEM.

be powered) and arrive at the cathode, where they reduce the oxidant ferricyanide Fe(III) into ferrocyanide Fe(II) or directly reduce O_2 . Ferrocyanide is then oxidized by O_2 , regenerating ferricyanide (not shown in Fig. 2). Thus the bioreagents PMS and ferricyanide are theoretically constantly regenerated and not consumed. Simultaneously, the protons accumulating inside the anode compartment diffuse across the PEM into the cathode compartment. The overall chemical reaction is



III. FABRICATION AND EXPERIMENT

The μ PEC was fabricated and assembled in the configuration of a polymer electrolyte fuel cell, as shown in Figs. 3 and 4. Low-stress nitride of 1300 Å was deposited by LPCVD on both sides of a Si wafer. The nitride was then patterned on the back side to define the electrode pads, flow ports, and bioreaction chamber [Fig. 3(a)], which were then formed by a through-wafer etch in KOH [Fig. 3(b)]. After stripping off the nitride in 49% HF, a Pyrex (7740) wafer was anodically bonded onto the front (polished) side of the Si wafer. Then, a 5 × 7 mm piece of Kapton tape was applied onto the Pyrex in the center of the chamber. The purpose of the Kapton was to mask that area of Pyrex during the subsequent evaporation of Cr/Au (500/2000 Å thick) onto the Si backside [Fig. 3(c)]. This Cr/Au film served as the electrode surface, with an area of about 1 cm² accessible to the reaction chambers after final assembly (described later).

The Si-Pyrex stack was then diced into 1 × 2 cm half-cells, and the Kapton tape was removed [Figs. 3(d) and 4(a)]. Micro-syringe needles (World Precision, Microfil 28 gauge, 250 μm ID) were glued to the ports of each half-cell to facilitate inlet and outlet flow; and Au wires were soldered onto the electrode pads. Finally, the μ PEC was assembled by sandwiching a

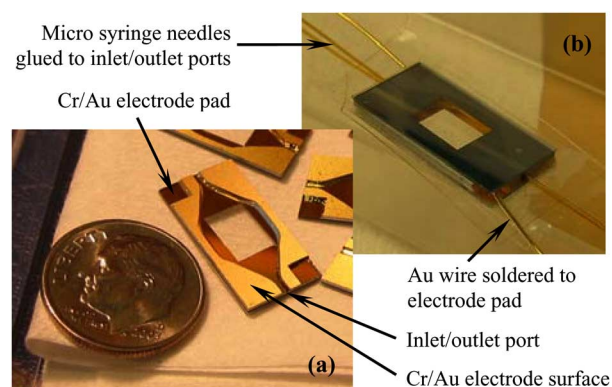


Fig. 4. (a) Half-cell before assembly; ref. Fig. 3(d). (b) Fully-assembled biosolar cell [see Fig. 3(e)]. The PEM and double-sided tape, pressed between the half-cells, are barely visible.

PEM (Nafion N-117, 183-μm thick) between 2 half-cells, with double-sided Scotch tape applied between the Cr/Au surface and PEM as a bonding agent and fluidic seal [Figs. 3(e) and 4(b)]. Before use, the Nafion PEM had been prepared in 80°C H_2O_2 , H_2SO_4 , and deionized water as described in [39]. After assembly, each bioreaction chamber (anode or cathode) enclosed a volume of about 0.05 cm³ = 50 μL.

Thylakoids were isolated from baby spinach using a procedure similar to [40], [41]—yielding 2.4 mg chlorophyll/mL, which was then suspended in 400 mM sucrose, 20 mM Tricine (pH 8.0), and 10 mM NaCl. This thylakoid mixture was then diluted into 50 mM Tricine (pH 8.0), 50 mM NaCl, 4 mM $MgCl_4$, and 300 μM PMS to a final volume of 10 mL, which resulted in an anode reaction mixture with 240 μg chlorophyll/mL. The cathode reaction mixture consisted of 20 mM potassium ferricyanide in deionized water. All chemicals were purchased from Sigma Aldrich and used as received. After preparation, the anode and cathode reaction mixtures were stored in syringes wrapped in aluminum foil and kept in ice until used. During the experiments, the anode and cathode reaction mixtures were pumped through their respective chambers of the μ PEC at 0.1 mL/min in counter-flowing directions. Two lighting conditions were imposed on the μ PEC: complete darkness or direct illumination of the anode compartment by a light source (a slide projector) calibrated to 2000 μmol photons/m²/s, which approximates the solar intensity during a cloudless, sunny day. All experiments were conducted at room temperature.

IV. RESULTS

A. Open Circuit Voltage, Current, Effect of Light Intensity

The open circuit voltage (OCV) performance of the μ PEC is shown in Fig. 5(a). In the dark, after flow was turned on, OCV climbed to 330 mV after 4 min; then, upon being subject to direct illumination of intensity 2000 μmol photons/m²/s, OCV sharply increased to and stabilized at 470 mV within 2 min. In repeated experiments, the maximum OCV under illumination with flow ranged from 440–480 mV (see also Fig. 5(b)). When darkness was again imposed (with flow still on), OCV returned to 330 mV. In control experiments in which either thylakoids or PMS was not added to the anode chamber reaction mixture,

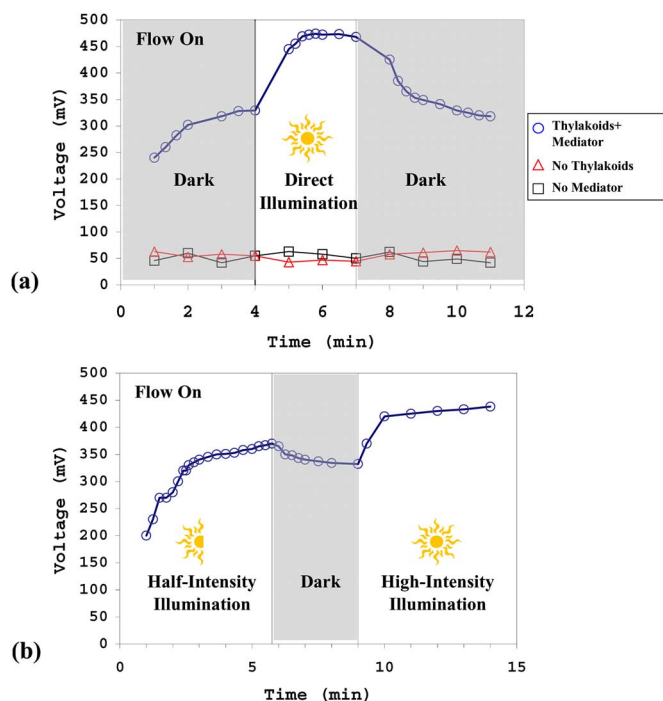


Fig. 5. (a) Open circuit voltage (OCV) under high-intensity direct illumination ($2000 \mu\text{mol photons/m}^2/\text{s}$): with and without thylakoids, mediator. (b) OCV under half-intensity direct illumination ($1000 \mu\text{mol photons/m}^2/\text{s}$). Flow of reaction mixtures through reaction chambers = 0.1.

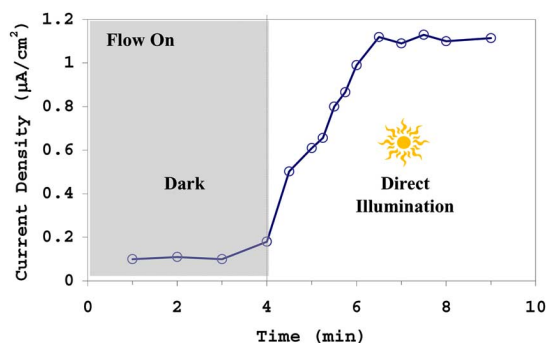


Fig. 6. Current density with load $R = 1 \text{ k}\Omega$. Direct illumination = $2000 \mu\text{mol photons/m}^2/\text{s}$.

negligible OCV of about 50–60 was measured (as also shown in Fig. 5(a)).

The effect of light intensity on OCV is illustrated in Fig. 5(b). OCV reached only 370 mV under half-intensity illumination ($1000 \mu\text{mol photons/m}^2/\text{s}$) but climbed to 440 mV under high intensity ($2000 \mu\text{mol photons/m}^2/\text{s}$), which is consistent with Fig. 5(a) under the same lighting conditions. This result demonstrates that the output level can be modulated by incident light intensity. Fig. 6 shows the current density, with a $1 \text{ k}\Omega$ load resistor, increased from $0.1 \mu\text{A}/\text{cm}^2$ in the dark to $1.1 \mu\text{A}/\text{cm}^2$ in about 2 min under direct illumination.

B. Effect of Flow

The flow of anode and cathode reaction mixtures through their respective chambers in the μPEC brings some noteworthy effects that are illustrated in Fig. 7. At time = 0, before flow was turned on and while in the dark, the OCV floated at about

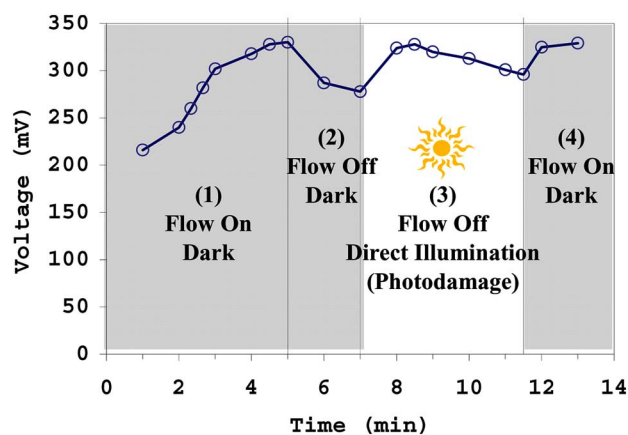


Fig. 7. Effect of flow and light on OCV.

60 mV (not shown). After flow was introduced (while still in the dark) and the both chambers were filled, OCV climbed to 330 mV within 5 min (Region 1 in Fig. 7). Why was the OCV nonzero even when there was no light? We conjecture that because the anodic reaction mixture was prepared under ambient lighting conditions, a certain concentration of PMS would have already been photosynthetically reduced by thylakoids even before it was pumped through the μPEC and subject to direct illumination. Thus, pumping an anode mixture with a certain concentration of already-reduced PMS through the μPEC would produce a nonzero OCV. However, as shown in Region 2 of Fig. 7, when the flow of “fresh” reaction mixtures was turned off while in the dark, OCV declined from 330 to 280 mV as the reduced PMS was gradually oxidized in the anode compartment.

In Region 3 of Fig. 7, direct illumination was switched on while flow was kept off. Here, the photosynthetic reactions of the photosystems “recharged” the PMS (Fig. 2) that had been oxidized in Region 2, causing OCV to climb back up to 320 mV—but only briefly. For within 2 minutes, the OCV again declined because: 1) under the intense illumination PSII suffered photo-oxidative damage and lacked the necessary compensation mechanisms [42]; and 2) with flow still off, fresh thylakoids with “active” (i.e., nondamaged) photosystems were not being supplied to the μPEC . Finally, in Region 4 of Fig. 7, the μPEC was again subject to darkness, but the flow was turned back on. Since these were the same conditions as Region 1, it is consistent that OCV returned to 330 mV within 2 min.

C. Power and Efficiency

The performance of the μPEC over a range of current densities is characterized in Fig. 8. As is characteristic of fuel cells [43], a tradeoff exists between operating voltage and power—power increases with current while operating voltage declines. For example, the highest power density of $5.4 \text{ pW}/\text{cm}^2$ at $1.1 \mu\text{A}/\text{cm}^2$ was achieved at the operating voltage of $5.2 \mu\text{V}$, which is less than the peak voltage of $6.7 \mu\text{V}$. Knowing the incident light intensity ($2000 \mu\text{mol photons/m}^2/\text{s}$) and using the relation $E = h\nu$ (where h is Planck’s constant and ν is the frequency of light), we calculated the efficiency of the μPEC to be 0.01% at the peak voltage of $6.7 \mu\text{V}$. Moreover, the electrical output of the μPEC was comparable to other

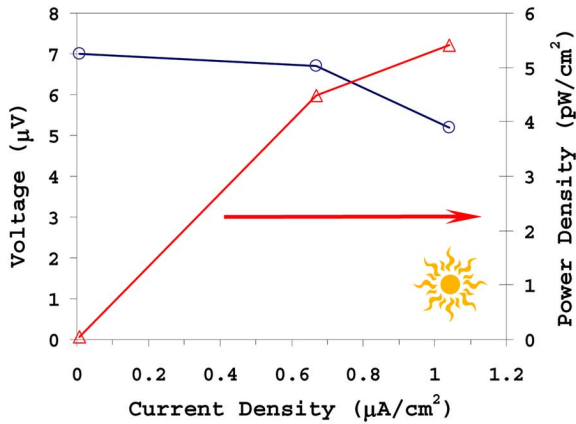


Fig. 8. Voltage and power density versus current density under direct illumination with flow.

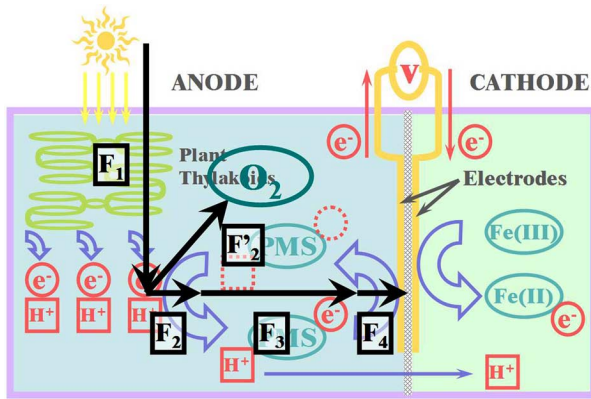


Fig. 9. Simple model of flux quantities, F_1 – F_4 , to estimate maximum current the biosolar cell can generate (see Fig. 2).

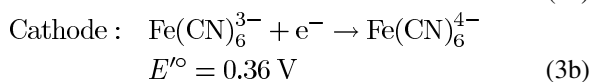
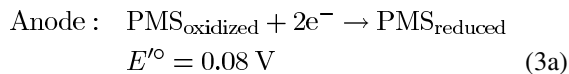
microfabricated biological fuel cells [6], [9], though generally lower than larger-scale biological fuel cells [44].

V. ESTIMATING OPEN CIRCUIT VOLTAGE AND CURRENT

Having discussed the performance of the μ PEC, we now describe simple first-order models for estimating open circuit voltage and current.

A. Open Circuit Voltage

As with conventional fuel cells, the open circuit voltage, $\Delta E'^{\circ}$, is determined by taking the difference between the standard reduction potentials, E'° , of the anode and cathode half reactions



$$\text{Ideal OCV: } \Delta E'^{\circ} = E'_{\text{cathode}} - E'_{\text{anode}}. \quad (3c)$$

Note that (3a) and (3b) compose the overall reaction (2). Using (3a)–(3c), the theoretical OCV $\Delta E'^{\circ} = 0.28 \text{ V}$, which is markedly less than the measured value of 0.47 V.

This difference can partially be reconciled by accounting for the relative concentrations of oxidized/reduced PMS and

ferricyanide/ferrocyanide in the respective chambers using the Nernst equation

$$E = E'^{\circ} + \frac{RT}{zF} \ln \frac{[\text{reactants}]}{[\text{products}]} \quad (4a)$$

where R is the gas constant, T is absolute temperature, z is the number of electrons in the redox reaction, and F is the Faraday constant. If it is assumed that most of the PMS is reduced by PSI (see Section V-B.2), then it may be approximated that $[\text{reactants}]/[\text{products}] = [\text{PMS}_{\text{oxidized}}]/[\text{PMS}_{\text{reduced}}] \approx 0.001$, so that $E_{\text{anode}} \approx -0.01 \text{ V}$ using (4a). Similarly, because the ferricyanide concentration is much greater than PMS, it may be assumed that most of the ferricyanide remain in the oxidized state, such that $[\text{reactants}]/[\text{products}] = [\text{Fe}(\text{CN})_6^{3-}]/[\text{Fe}(\text{CN})_6^{4-}] \approx 1000$, with the result that $E_{\text{cathode}} \approx 0.45 \text{ V}$. Thus, a more realistic estimate of the actual OCV is

$$\text{OCV: } \Delta E = E_{\text{cathode}} - E_{\text{anode}} = 0.46 \text{ V} \quad (4b)$$

which is a better approximation for the measured OCV of 0.47 V. Nonetheless, this is still a simplistic estimate that does not account for other factors such differences in pH and ionic concentrations between the two chambers.

B. Current

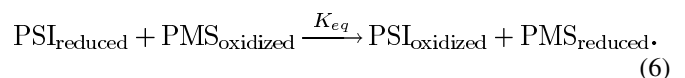
We now present a simple first-order model to estimate the maximum current density that the μ PEC can generate and to elucidate the major loss mechanisms that limit current density. This model is shown in Fig. 9, where the current density generated is represented as a series of photon or electron fluxes F_1 – F_4 superimposed on Fig. 2. Each of these flux processes will now be described and its impact on current assessed.

1) F_1 : *Flux and Absorbance of Incident Photons*: The ultimate energy source for the current that the μ PEC generates is from the flux of incident photons—that is, the direct illumination of $f_0 = 2000 \mu\text{mol photons/m}^2/\text{s} = 1.2 \times 10^{17} \text{ photons/cm}^2/\text{s}$. As a first-order estimate, assuming for simplicity that the μ PEC absorbs all of this photon flux and using the fact that 1 electron is transported through the photosystems per 2 photons absorbed [Fig. 1(c)] [38], we find the maximum possible current density as

$$F_1 = i_{\text{max}} = f_0 \cdot \frac{1 \text{ electron}}{2 \text{ photons}} \cdot \frac{q}{\text{electron}} = 9.6 \frac{\text{mA}}{\text{cm}^2} \quad (5)$$

where $q = 1.602 \times 10^{-19} \text{ C}$. Since the maximum measured current density of $1.1 \mu\text{A/cm}^2$ is almost four orders of magnitude less than F_1 , losses must be occurring in one or more of the other flux quantities.

2) F_2 : *Transfer of Electrons From Photosystem I to PMS_{ox}*: The quantity F_2 characterizes the transfer of electrons from Photosystem I (PSI) to the oxidized form of PMS

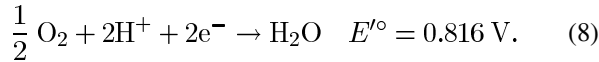


In (6), K_{eq} is the equilibrium constant of the reaction and is calculated using a form of the Nernst Equation [38]:

$$K_{eq} = \exp\left(\frac{zF}{RT}\Delta E'^o\right) \quad (7)$$

where R is the gas constant; F is the Faraday constant; T is the absolute temperature; $z = 2$, the number of electrons involved in reaction (6); and $\Delta E'^o$ is calculated using a relationship similar to (4). Skipping the details, we find that $K_{eq} = 2 \times 10^{20} \gg 1$, which implies that the transfer of electrons from PSI to PMS_{ox} is highly favorable thermodynamically. Therefore, we expect that $F_2 \approx F_1$ and that electron transfer to PMS_{ox} is likely not the bottleneck limiting the current.

3) F_2' : *Oxidation of Ferredoxin or PMS Re by O₂*: Oxygen (O₂) is a strong oxidant and easily combines with e⁻ and H⁺ to yield H₂O, as indicated by the high reduction potential E'^o of the reaction



The typical concentration of O₂ dissolved in water is about 5 mg/L = 156 μM, which is comparable to the 300 μM of PMS used in these experiments. So we expect that O₂ competes strongly with PMS_{ox} to oxidize ferredoxin from PSI and that O₂ oxidizes even PMS_{re} to a certain degree. The result is that some electrons never make it to the electrode as current. Thus, oxidation by O₂ is likely one of the factors that limits available current. Despite this, though initially attempted, no facility was implemented to exclude O₂ from the anode chamber (e.g., by N₂ bubbling) because the small, flat volume of the MEMS-fabricated anode chamber (~0.05 cm³) meant that, for example, N₂ bubbling would have significantly disrupted the flow of the bioreaction mixture.

4) F_3 : *Diffusion of PMS_{re} to Electrode Surface*: Since reduced PMS carries the electrons, the diffusion rate of PMS_{re} to the electrode surface strongly correlates with the current density that the μPEC can sustain. As a first-order approximation, we apply Fick's First Law

$$F_{PMS} = -D_{PMS} \frac{\partial C}{\partial x} \approx D_{PMS} \frac{\Delta C}{\Delta x} \quad (9)$$

where D_{PMS} is the diffusivity of PMS in solution, which can be conservatively approximated by the diffusivity of O₂ in water, $D_{PMS} \approx D_{O_2} \approx 10^{-5} \text{ cm}^2/\text{s}$. In addition, while PMS molecules are distributed throughout the anode chamber, we assume for simplicity that all PMS are concentrated in a plane halfway between the Pyrex/Cr/Au electrode surface and the Nafion PEM. Under these assumptions, $\Delta C = 300 \mu\text{M} = 1.8 \times 10^{17} \text{ cm}^{-3}$ and $\Delta x = 250 \mu\text{m}$. Employing (9), the current density that can be sustained by PMS_{re} diffusion is

$$F_3 = i_{\text{diff}} = F_{PMS} \cdot \frac{2 \text{ electrons}}{1 \text{ PMS}} \cdot \frac{q}{\text{electron}} = 23 \frac{\mu\text{A}}{\text{cm}^2}. \quad (10)$$

Because F_3 is within an order of magnitude of the 1.0 μA/cm² peak current density measured, we surmise that PMS diffusion is one of the major factors limiting current.

5) F_4 : *Transfer of Electrons From PMS_{re} to Electrode*: To simplify the analysis, we assume that all reduced PMS molecules that impinge the Cr/Au electrode surface donate their electrons. In this way, F_4 also is not a major factor limiting current.

Finally, we note that the concentration of the ferricyanide electron acceptor in the cathode chamber (20 mM) is much greater than that of the PMS electron donator (300 μM) in the anode compartment. So we surmise that the kinetics in the cathode chamber do not significantly limit the current.

VI. CONCLUSION

From the foregoing, we conclude that, under lossless conditions and illumination of 2000 μmol photons/m²/s, the μPEC would be able to generate a theoretical maximum current density of about $i_{\text{max}} = 9.6 \text{ mA}/\text{cm}^2$. However, the measured maximum of 1.0 μA/cm² at 5.2 μV under illumination falls short of the theoretical value, primarily because of two loss mechanisms: (1) the "low" diffusion rate of electron-carrying PMS to the electrode surface and (2) the scavenging of electrons by O₂ from Photosystem I (ferredoxin) and reduced PMS. These loss mechanisms are also responsible for the poor efficiency of 0.01%. The measured open circuit voltage under illumination was 470 mV; and in the dark the μPEC continued to produce power using reduced equivalents generated during illumination, yielding 330 mV OCV. These current and OCV levels are comparable to other microfabricated biological fuel cells.

We anticipate being able to reduce the effect of these loss mechanisms and thus increase output and efficiency by immobilizing biocatalysts (i.e., PMS and ferricyanide) and thylakoids onto the anode and cathode surface [47]. Work by Katz *et al.* on enzymatic fuel cells has demonstrated certain immobilized biocatalysts that increase current density by two orders of magnitude and render the biocatalysts to be insensitive to electron scavenging by O₂ [44], [48], [49]. Furthermore, as already partially demonstrated, we may affect the electrical output by optimizing illumination intensity, flow rate, and concentrations of the components in the anode and cathode reaction mixtures.

ACKNOWLEDGMENT

The devices presented in this paper were fabricated in the University of California (UC), Berkeley, Microfabrication Laboratory. The experiments were performed in Prof. A. Melis' photosynthesis laboratory in the Department of Plant and Microbial Biology at UC Berkeley.

REFERENCES

- [1] B. Warneke, M. Last, B. Liebowitz, and K. S. J. Pister, "Smart dust: Communicating with a cubic-millimeter computer," *Computer*, vol. 34, pp. 44–51, 2001.
- [2] B. A. Warneke and K. S. J. Pister, "Smart dust mote forerunners," in *Proc. IEEE Conf. Microelectromechanical Systems*, Interlaken, Switzerland, 2001, pp. 357–360.
- [3] S. E.-A. Hollar, A. Flynn, C. Bellew, and K. S. J. Pister, "Solar powered 10 mg silicon robot," in *Proc. IEEE Conf. Microelectromechanical Systems*, Kyoto, Japan, 2003, pp. 706–711.

- [4] S. E.-A. Hollar, A solar-powered, milligram prototype robot from a three-chip process. Berkeley, CA, Dept. Elec. Eng. Comp. Sci., Univ. California. Berkeley, CA, 2003, Ph.D. dissertation.
- [5] K. B. Lam, E. Johnson, and L. Lin, "A bio-solar cell powered by sub-cellular plant photosystems," in *Proc. IEEE Conf. Microelectromechanical Systems*, Maastricht, The Netherlands, 2004, pp. 220–223.
- [6] K. B. Lam, M. Chiao, and L. Lin, "A micro photosynthetic electrochemical cell," in *Proc. IEEE Conf. Microelectromechanical Systems*, Kyoto, Japan, 2003, pp. 391–394.
- [7] S. C. Kelley, G. A. Deluga, and W. H. Smyrl, "A miniature methanol/air polymer electrolyte fuel cell," *Electrochem. Solid-State Lett.*, vol. 3, pp. 407–407, 2000.
- [8] —, "Miniature fuel cells fabricated on silicon substrates," *AICHE J.*, vol. 48, pp. 1071–1081, 2002.
- [9] M. Chiao, K. B. Lam, and L. Lin, "A microfabricated microbial fuel cell," in *Proc. IEEE Conf. on Microelectromechanical Systems*, Kyoto, Japan, 2003, pp. 383–386.
- [10] M. Chiao, K. B. Lam, Y.-C. Su, and L. Lin, "A miniaturized microbial fuel cell," in *Proc. Solid-State Sensors and Actuators Workshop*, Hilton Head Island, SC, 2002.
- [11] K. Tanaka, N. Kashiwagi, and T. Ogawa, "Effects of light on the electrical output of bioelectrochemical fuel-cells containing anabaena variabilis M-2 mechanisms of the post-illumination burst," *J. Chem. Tech. Biotechnol.*, vol. 42, pp. 235–240, 1988.
- [12] K. Tanaka, R. Tamamushi, and T. Ogawa, "Bioelectrochemical fuel cells operated by the cyanobacterium anabaena variabilis," *J. Chem. Tech. Biotechnol. B, Biotechnol.*, vol. 35, pp. 191–197, 1985.
- [13] T. Yagishita, T. Horigome, and K. Tanaka, "Effects of light, CO₂, and inhibitors on the current output of biofuel cells containing the photosynthetic organism synechococcus sp," *J. Chem. Technol. Biotechnol.*, vol. 56, pp. 393–399, 1993.
- [14] —, "Biofuel-cells containing photosynthetic microorganisms," *J. Electrochem. Soc. Jpn.*, vol. 61, pp. 687–688, 1993.
- [15] T. Yagishita, S. Sawayama, K.-I. Tsukahara, and T. Ogi, "Photosynthetic bio-fuel cell using cyanobacteria," *Renewable Energy*, vol. 9, pp. 958–961, 1996.
- [16] —, "Performance of photosynthetic electrochemical cells using immobilized anabaena variabilis M-3 in discharge/culture cycles," *J. Ferment. Bioeng.*, vol. 85, pp. 546–549, 1998.
- [17] —, "Effects of intensity of incident light and concentrations of synechococcus sp. and 2-hydroxy-1,4-naphthoquinone on the current output of photosynthetic electrochemical cell," *Solar Energy*, vol. 61, pp. 347–353, 1997.
- [18] —, "Effects of glucose addition and light on current outputs in photosynthetic electrochemical cells using synechocystis sp. Pcc6714," *J. Biosci. Bioeng.*, vol. 99, pp. 210–214, 1999.
- [19] S. Tsujimura, A. Wadano, K. Kano, and T. Ikeda, "Photosynthetic bioelectrochemical cell utilizing cyanobacteria and water-generating oxidase," *Enzyme Microb. Technol.*, vol. 29, pp. 225–231, 2001.
- [20] E. L. Gross, D. R. Youngman, and S. L. Winemiller, "An FMN-photosystem I photovoltaic cell," *Photochem. Photobiol.*, vol. 28, pp. 249–256, 1978.
- [21] R. Bhardwaj, R. L. Pan, and E. L. Gross, "Solar energy conversion by chloroplast photochemical cells," *Nature*, vol. 289, pp. 396–398, 1981.
- [22] —, "A photosystem I-phenosafranine solar cell," *Photochem. Photobiol.*, vol. 34, pp. 215–222, 1981.
- [23] R. L. Pan, I. J. Fan, R. Bhardwaj, and E. L. Gross, "The photosynthetic photoelectrochemical cell using flavin mononucleotide as the electron acceptor," *Photochem. Photobiol.*, vol. 35, pp. 655–664, 1982.
- [24] R. L. Pan, R. Bhardwaj, and E. L. Gross, "Photosynthetic photoelectrochemical cell," *Biophysical J.*, vol. 33, pp. 59a–59a, 1981.
- [25] M. Aizawa, M. Hirano, and S. Suzuki, "Photoelectrochemical energy conversion system modeled on the photosynthetic process," *Electrochim. Acta.*, vol. 23, pp. 1185–1190, 1978.
- [26] —, "Photo-induced electron transfer of a chlorophyll-liquid crystal electrode to water," *Electrochim. Acta.*, vol. 23, pp. 1061–1065, 1978.
- [27] —, "Photoelectrochemical oxygen evolution from water by a manganese chlorophyll-liquid crystal electrode," *Electrochim. Acta.*, vol. 24, pp. 89–94, 1978.
- [28] L. A. Drachev, A. A. Kondrashin, V. D. Samuilov, and V. P. Skulachev, "Generation of electric potential by reaction center complexes from *Rhodospirillum rubrum*," *FEBS Lett.*, vol. 50, pp. 219–222, 1975.
- [29] L. A. Drachev, A. A. Jasaitis, A. D. Kaulen, A. A. Kondrashin, L. V. Chu, A. Y. Semenov, I. I. Severina, and V. P. Skulachev, "Reconstitution of biological molecular generators of electric current: Cytochrome oxidase," *J. Biol. Chem.*, vol. 251, pp. 7072–7076, 1976.
- [30] E. L. Barsky, Z. Dancshazy, L. A. Drachev, M. D. Il'ina, A. A. Jasaitis, A. A. Kondrashin, V. D. Samuilov, and V. P. Skulachev, "Reconstitution of biological molecular generators of electric current: Bacteriochlorophyll and plant chlorophyll complexes," *J. Biol. Chem.*, vol. 251, pp. 7066–7071, 1976.
- [31] N. K. Packham, D. M. Tiede, P. Mueller, and P. L. Dutton, "Construction of a flash-activated cyclic electron transport system by using bacterial reaction centers and the ubiquinone-cytochrome b-c₁/c segment of mitochondria," *Proc. Natl. Acad. Sci.*, vol. 77, pp. 6339–6343, 1980.
- [32] N. K. Packham, C. Packham, P. Mueller, D. M. Tiede, and P. L. Dutton, "Reconstitution de photochemically active reaction centers in planar phospholipid membranes," *FEBS Lett.*, vol. 110, pp. 101–106, 1980.
- [33] A. F. Janzen, "Photoelectrochemical conversion using reaction-centre electrodes," *Nature*, vol. 286, pp. 584–585, 1980.
- [34] W. Haehnel, A. Heupel, and D. Hengstermann, "Investigations on a galvanic cell driven by photosynthetic electron transport," *Zeitschrift fur Naturforschung C-A Journal of Biosciences*, vol. 33, pp. 392–401, 1978.
- [35] W. Haehnel and H. J. Hockheimer, "On the current generated by a galvanic cell driven by photosynthetic electron transport," *Bioelectrochem. Bioeng.*, vol. 6, pp. 563–574, 1979.
- [36] W. Haehnel, "Photosynthetic electron transport in higher plants," *Ann. Rev. Plant. Physiol.*, vol. 35, pp. 659–693, 1984.
- [37] M. J. Allen and A. E. Crane, "Null potential voltammetry—An approach to the study of plant photosystem," *Bioelectrochem. Bioeng.*, vol. 3, pp. 84–91, 1976.
- [38] D. L. Nelson and M. M. Cox, *Lehninger Principles of Biochemistry*, 3rd, Ed. New York: Worth, 2000, pp. 691–714.
- [39] S. J. Lee, "Effects of nafion impregnation on performance of pemfc electrodes," *Electrochimica Acta.*, vol. 43, pp. 3693–3701, 1998.
- [40] A. Melis, *Plant and Microbial Biology 135: Physiology and Biochemistry of Plants Laboratory Manual*. Berkeley, CA: Univ. California Press, 2003.
- [41] S. P. Berg, *Plant Physiology: Photosynthesis Laboratory Protocol*. Winona, MN: Minnesota State Univ. Winona (Winona State Univ.) Press, 2004.
- [42] E. M. Aro, I. Virgin, and B. Andersson, "Photoinhibition of photosystem ii. Inactivation, protein damage and turnover," *Biochim. Biophys. Acta.*, vol. 1143, pp. 113–134, 1993.
- [43] *Fuel Cells: A Handbook*, 5 ed. Morgantown, WV: U.S. Dep. Energy/Parsons, Inc., EG&G Services, 2000.
- [44] E. Katz, A. N. Shipway, and I. Willner, "Biochemical fuel cells," in *Handbook of Fuel Cells—Fundamentals, Technology and Applications*, W. Vielstich, A. Lamm, and H. A. Gasteiger, Eds. Chichester, U.K.: Wiley, 2003, vol. 355–381.
- [45] ImmunoPure PMS (Product). Rockford, IL, Pierce Chemical Company, 2000.
- [46] *CRC Handbook of Biochemistry and Molecular Biology*. Boca Raton, FL, CRC Press, 1975.
- [47] K. B. Lam, E. F. Irwin, K. E. Healy, and L. Lin, "Bioelectrocatalytic self-assembled thylakoids for micro power and sensing applications," *Sens. Actuators B, Chem.*, vol. 117, pp. 480–487, 2006.
- [48] A. Bardea, E. Katz, A. F. Buckmann, and I. Willner, "NAD⁺-dependent enzyme electrodes: Electrical contact of cofactor-dependent enzymes and electrodes," *J. Amer. Chem. Soc.*, vol. 119, pp. 9114–9119, 1997.
- [49] I. Willner, V. Heleg-Shabtai, R. Blonder, E. Katz, and G. Tao, "Electrical wiring of glucose oxidase by reconstitution of FAD-modified monolayers assembled onto Au-electrodes," *J. Amer. Chem. Soc.*, vol. 118, pp. 10321–10322, 1996.



Kien Bang Lam received the B.S. degree in mechanical engineering from the University of California, Berkeley (UCB), in 1997, the M.S. degree in mechanical engineering at the University of Michigan, Ann Arbor, in 1999, and the Ph.D. in mechanical engineering from UCB, in 2005.

He is currently a Senior R&D Process Engineer with Intel Corporation, Santa Clara, CA. Previously, he was a Mechanical Engineer at Applied Materials in Santa Clara, CA, from 1999 to 2001; an Intern Researcher at Ford Research Laboratory, Dearborn, MI,

from 1998 to 1999; a Graduate Student Researcher in the Mechanical Engineering Department at the University of Michigan, Ann Arbor, from 1997 to 1999; and an Intern at Lawrence Berkeley National Laboratory, Berkeley, CA, from 1996 to 1997.

Eric A. Johnson received the B.A. degree in biology and the B.S. degree in chemical engineering from the University of Kansas, Lawrence, in 1994. He worked as a Research Technician for Merck Research Laboratories, Lawrence, KS, before attending graduate school at Johns Hopkins University, Baltimore, MD, where he received the Ph.D. degree in biochemistry in 2000.

In 2001, he was awarded a National Science Foundation Postdoctoral Fellowship in microbial biology, which he used to study the photosynthetic and hydrogen-producing metabolism of *C. reinhardtii* at the University of California, Berkeley. He is currently a Postdoctoral Fellow at Johns Hopkins University, where he is pursuing protein engineering of photosynthetic enzymes of *C. reinhardtii*.



Mu Chiao received the B.S. and M.S. degrees from National Taiwan University, Taiwan, in 1996, and the Ph.D. degree in mechanical engineering from the University of California, Berkeley, in 2002.

From August 2002 to February 2003, he was with the Berkeley Sensor and Actuator Center, University of California at Berkeley, as a Postdoctoral Research Fellow. His research effort was on MEMS power source and nanowire/tube synthesis. From March 2003 to July 2003, he was a Senior MEMS Engineer with Intpax, Inc., San Jose, CA, working on MEMS sensors for automotive applications. He has been with the Department of Mechanical Engineering, The University of British Columbia, Canada, since 2003 as an Assistant Professor. His current research interests include design and fabrication of MEMS and nanodevices for biomedical applications.

Dr. Chiao is the recipient of the Canada Research Chairs, Tier 2 program.



Liwei Lin (S'92–M'93) received the B.S. degree in power mechanical engineering from National Tsing Hua University, Taiwan, and the M.S. and Ph.D. degrees in mechanical engineering from the University of California, Berkeley (UCB), in 1986, 1991, and 1993, respectively.

He joined UCB in 1999, and is now Chancellor's Professor in the Mechanical Engineering Department and co-Director at the Berkeley Sensor and Actuator Center. He was an Associate Professor in the Institute of Applied Mechanics, National Taiwan University, Taiwan (1994–1996), and an Assistant Professor in the Mechanical Engineering Department, the University of Michigan, Ann Arbor (1996–1999).

His research interests are in design, modeling, and fabrication of micro/nanostructures, micro/nanosensors, and micro/nanoactuators as well as mechanical issues in micro/nanosystems including heat transfer, solid/fluid mechanics, and dynamics. He has eight issued U.S. patents in the area of MEMS.

Dr. Lin was the recipient of the 1998 National Science Foundation CAREER Award for research in MEMS Packaging and the 1999 *ASME Journal of Heat Transfer* Best Paper Award for his work on micro scale bubble formation. Currently, he serves as a Subject Editor for the *IEEE/ASME JOURNAL OF MICROELECTROMECHANICAL SYSTEMS* and the North and South America Editor of *Sensors and Actuators—A Physical*. He led the effort to establish the MEMS division in ASME, and served as the founding Chairman of the Executive Committee from 2004–2005.